

## Research Paper

# Structural Parametric Study of a Piezoelectric Energy Harvester for a Specific Excitation Frequency of an Electric Motor, Considering Fatigue Life

Ping YANG<sup>(1),(2)</sup>, Nabil MOHAMAD USAMAH<sup>(1)</sup>, Abdullah Aziz SAAD<sup>(1)</sup>,  
Ahmad Zhafran AHMAD MAZLAN<sup>(1)\*</sup> 

<sup>(1)</sup> *School of Mechanical Engineering, Engineering Campus, Universiti Sains Malaysia*  
Penang, Malaysia

<sup>(2)</sup> *College of Intelligent Manufacturing and Automobile, Chongqing Technology and Business College*  
Chongqing, China

\*Corresponding Author e-mail: [zhafran@usm.my](mailto:zhafran@usm.my)

*Received May 8, 2024; revised January 9, 2025; accepted April 9, 2025;*  
*published online June 6, 2025.*

Over the past decade, extensive research has been conducted in the field of piezoelectric energy harvesting, which drives advancements in novel designs and techniques. In this study, the vibration of an electric motor is characterized, and a piezoelectric energy harvester (PEH) beam with a natural frequency of 50 Hz is designed and fabricated. Then, the electromechanical characteristics of the PEH are simulated and tested through both finite element simulation and experiment. The validated simulation model can accurately predict the vibration characteristics of the PEH, which can be utilized for design improvements. Based on this beam structure, three sets of PEHs with different sizes are designed. A study of the output voltage and fatigue life of these different PEH sizes is conducted, and the relationship between the electromechanical coupling effect and its varying values is discussed. Based on the results, design schemes ①~⑥ demonstrate advantages in terms of output voltage efficiency and fatigue strength, making them suitable for various environments and application purposes. This study establishes an efficient method for analyzing the structural parametric performance of piezoelectric cantilever beams, which paves the way for future research on fatigue-based structural design guidelines for PEH in electric motors.

**Keywords:** piezoelectric energy harvester (PEH); fatigue; output voltage; vibration.



Copyright © 2025 The Author(s).  
This work is licensed under the Creative Commons Attribution 4.0 International CC BY 4.0  
(<https://creativecommons.org/licenses/by/4.0/>).

## 1. Introduction

Intelligent devices in the current digital era require constant monitoring to ensure long-term operation and functionality, establish operational profiles, and anticipate specific malfunctions. Electrical devices generate minor wideband vibrations during regular operation. Before malfunctions occur, oscillations that cause variations in displacement, frequency, and other related parameters can be distinguished from steady-state operations. Multiple sensors are needed to monitor the devices during operation, and it has become common to seek an appropriate power source from these elec-

trical devices. At present, the most promising method for powering wireless sensors is to capture the vibration energy produced by the device itself. The vibration frequencies generated by these devices are generally in the power spectrum and harmonic waves. This study focuses on the optimal design of an piezoelectric energy harvester (PEH) for 50 Hz vibrations excited by an electric motor, with the objective of increasing energy output while also improving the structure's durability.

Piezoelectric materials have the ability to convert mechanical vibration energy into electrical energy and have been widely investigated for energy harvesting

due to their high energy density (LI, LEE, 2022). Piezoelectric energy harvesting is a burgeoning topic that has been investigated for use in construction, machinery, automobiles, and aerospace, owing to the significant amount of wasted vibration energy produced by these systems. These devices are frequently utilized as a power source for self-powered wireless sensors and employed in situations where external power is unavailable and using batteries is not a practical solution. The initial application of PEH was presented by PANDA *et al.* (2022), where a lead zirconate titanate (PZT) patch was attached to the root of a cantilever beam.

Piezoelectric elements may experience considerable deformation due to the cantilever beam's ability to modify the frequency and increase the vibration amplitude when a mass block is applied. This configuration is currently the most widely used because of its ease of implementation, high efficiency, and well-developed technology. Extensive research has been carried out over the past two decades on the design, functionality, and application of cantilever beam piezoelectric harvesters. ZHANG *et al.* (2022) indicated that vibration-based PEHs may produce maximum power when operated at the resonant frequency, and the power output drops dramatically as the natural frequency of the PEH deviates from the vibration frequency. According to RAFIQUE and BONELLO (2010), it was found that the resonant frequency of the cantilever beam is negatively correlated with its length while its thickness is positively correlated with the resonance frequency. When the vibration characteristics of the PEH match the vibration frequency of the surrounding environment, the harvester will undergo multi-modal resonance, resulting in significant deformation and causing large stress and strain at the end of the cantilever beam. The harvester's lifespan may be impacted over time by fatigue damage due to the prolonged concentration of stress and strain. Additionally, the output voltage is proportional to its length and inversely proportional to its width and thickness (WANG *et al.*, 2019).

To match the low-frequency vibrations of the surroundings and increase the PEH output voltage, the cantilever beam's length and mass must also be increased, or its width and thickness need to be decreased. However, ROUNDY *et al.* (2005) concluded that as the aspect ratio increases (as natural frequencies differ across structures), the strain at the root of the cantilever beam changes drastically, causing the overall deformation of the piezoelectric layer to increase. As a result, the piezoelectric layer experiences an increase in stress, which has a substantial effect on its fatigue life.

Relevant research has indicated that fatigue life and output voltage are incompatible and cannot be optimized by a single variable. Current research has de-

voted considerable effort to optimizing the structure of energy harvesters based on structural strain and material strength to improve energy harvesting conversion efficiency and power output. Few studies address the contradictions between fatigue damage and output voltage caused by structural parameters. However, there are almost no references studying the coupling effects of multiple variables on output voltage and fatigue life. A few commercially PEHs are available, but they are limited by a narrow bandwidth of operational frequency and concerns regarding the reliability and durability of the structure.

Although numerous studies have investigated the structural parametric and fatigue-related issues of PEH, most have focused on the impact of a single variable on either output voltage or fatigue life. There are not many studies that systematically examine and discuss the relationships among structural size, fatigue damage, and output voltage. Moreover, most research adopts the approach of matching external vibration excitation to the natural frequency of the structure, rather than adjusting the structure's inherent frequency to match a specific external vibration source. However, modifying a single variable can cause changes in the natural frequency of the structure, limiting the practical value of comparing the performance of structures with different natural frequencies in a consistent vibration environment in terms of energy absorption. The most important aspect of designing a PEH beam to match a specific surrounding frequency is to examine the combine influence of multiple variables. These relationships do not have a simple linearly increasing or decreasing relationship, and a practical approach is required to optimize appropriate structural dimensions.

To address this gap, the main aim of this study is to design PEHs integrated into an electric motor by evaluating their energy output and fatigue life, using PEHs with similar natural frequencies but different sizes through laboratory testing and numerical simulation. Then, the optimal design of PEH beams is determined to achieve an optimal balance between fatigue damage and maximum output voltage. This work is organized into six major sections. First, the background, and recent advances in PEHs are reviewed. The second section introduces the electro-mechanical model and the energy harvesting system. In Sec. 3, the dynamic characteristics of the motor and PEH beams with a natural frequency of 50 Hz of natural frequencies are measured and developed, and their electro-mechanical characteristics are then examined using both ANSYS software and experimental validation. In Sec. 4, three sets of PEHs are theoretically modeled, their output voltages and maximum stress are simulated, and five beams are selected for further analysis. In Sec. 5, the fatigue life of the selected beams is calculated, and the design strategies under different usage

environments are discussed. The conclusion summarizes the major findings and the research value of this work.

## 2. Electro-mechanical model of PEH

Currently, the most commonly used PEH structure is the cantilever beam type (SEZER, KOÇ, 2021), mainly composed of a piezoelectric layer, a beam, and a mass block, as shown in Fig. 1.

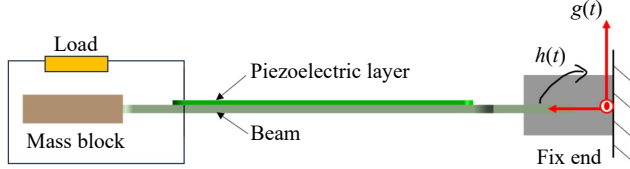


Fig. 1. Piezoelectric cantilever beam model.

Assume that the length of the piezoelectric cantilever beam is  $L$ , width is  $b$ , thickness of the piezoelectric layer is  $H$ , thickness of the elastic substrate layer is  $D$ , and the mass block weight is  $M$ . The system is subjected to translational excitation  $g(t)$  and a small rotational excitation  $h(t)$  at the base. Due to the large aspect ratio of the beam, the effects of shear deformation and rotational inertia of the beam are neglected, and the beam is treated as an equivalent Euler–Bernoulli beam. The free vibration equation of the piezoelectric beam can be expressed as (FENG *et al.*, 2023)

$$E \frac{\partial^4 w(x, t)}{\partial^4 x} + m \frac{\partial^2 w(x, t)}{\partial t^2} = 0, \quad (1)$$

where  $E$  represents the bending stiffness of the piezoelectric beam,  $m$  is the mass per unit length of the piezoelectric beam, and  $w(x, t)$  represents the transverse displacement at position  $x$  along the beam's neutral axis relative to the fixed inertial system. The transverse vibration displacement of the piezoelectric cantilever beam can be expressed as

$$w(x, t) = w_b(x, t) + w_{\text{rel}}(x, t), \quad (2)$$

where  $w_b(x, t)$  is the base excitation displacement, and  $w_{\text{rel}}(x, t)$  is the displacement relative to the fixed end. Considering the electromechanical coupling effect, the dynamic equation of the piezoelectric cantilever beam can be further written as

$$\begin{aligned} E \frac{\partial^4 w_{\text{rel}}(x, t)}{\partial^4 x} + c_s I \frac{\partial^5 w_{\text{rel}}(x, t)}{\partial^4 x \partial t} \\ + c_a \frac{w_{\text{rel}}(x, t)}{\partial t} + m \frac{\partial^2 w_{\text{rel}}(x, t)}{\partial t^2} + \xi V_0(t) \\ = -[m + M\delta(x - L)] \frac{\partial^2 w_b(x, t)}{\partial t^2}, \end{aligned} \quad (3)$$

where  $c_s$  is the strain damping coefficient,  $c_a$  is the air viscoelastic damping coefficient, and  $\xi$  is the electromechanical coupling coefficient. Using the modal superposition method, the solution to Eq. (3) can be written as

$$w_{\text{rel}}(x, t) = \sum_{r=1}^{\infty} \varphi_r(x) q_r(t), \quad (4)$$

where  $\varphi_r(x)$  is the normalized mode shape function for the  $r$ -th mode of the piezoelectric cantilever beam, and  $q_r(t)$  is the corresponding generalized modal coordinate. Solving Eq. (4) yields the relative vibration response of the beam:

$$\begin{aligned} w_{\text{rel}}(x, t) = \alpha e^{j\omega t} \sum_{r=1}^{\infty} \frac{\omega^2 G_0 [m\gamma_r^\omega + M\varphi_r(L) - X_r V_m]}{\omega_r^2 - \omega^2 + j2\zeta_r \omega_r \omega} \\ \cdot \left[ \cos \frac{\lambda_r}{L} x - \cosh \frac{\lambda_r}{L} x \right. \\ \left. + K \left( \sin \frac{\lambda_r}{L} x - \sinh \frac{\lambda_r}{L} x \right) \right], \end{aligned} \quad (5)$$

where

$$\gamma_r^\omega = \int_0^L \varphi_r(x) dx, \quad (6)$$

$G_0$  is the base excitation displacement amplitude,  $\omega$  is the excitation frequency,  $j$  is the imaginary unit,  $\lambda_r$  is the dimensionless frequency of the  $r$ -th mode,  $\alpha$  is the modal amplitude constant,  $\omega_r$  is the undamped natural frequency of the  $r$ -th mode,  $X_r$  is the modal electromechanical coupling coefficient,  $\zeta_r$  is the mechanical damping ratio,  $V_m$  is the voltage amplitude, and the expression for  $K$  is:

$$K = \frac{\sin \lambda_r - \sinh \lambda_r + \lambda_r \frac{M}{mL} (\cos \lambda_r - \cosh \lambda_r)}{\cos \lambda_r + \cosh \lambda_r - \lambda_r \frac{M}{mL} (\sin \lambda_r - \sinh \lambda_r)}. \quad (7)$$

According to Kirchhoff's law and the electrical response equation, the expression for the power output of the piezoelectric cantilever beam can be written as

$$P(t) = \frac{V^2(t)}{R} = \frac{1}{R} \left( \frac{\sum_{r=1}^{\infty} \mu_r \frac{j\omega^3 [m\gamma_r^\omega + M\varphi_r(L)]}{\omega_r^2 - \omega^2 + j2\zeta_r \omega_r \omega}}{\sum_{r=1}^{\infty} \frac{j\omega X_r \mu_r}{\omega_r^2 - \omega^2 + j2\zeta_r \omega_r \omega} + \frac{j\omega\psi + 1}{\psi}} G_0 e^{j\omega t} \right)^2, \quad (8)$$

where

$$\psi = \frac{R\epsilon_{33}^s bL}{H}, \quad (9)$$

$$\mu_r = \frac{-d_{31} Y_p e H}{\epsilon_{33}^s L} \frac{d\varphi_r(x)}{dx} \Big|_{x=L}, \quad (10)$$

$$\epsilon_{33}^s = \epsilon_{33}^t - d_{31}^2 Y_p, \quad (11)$$

where  $Y_p$  is the elastic modulus of the piezoelectric layer,  $d_{31}$  is the piezoelectric constant,  $e$  is the distance

from the middle layer of the piezoelectric cantilever beam to the neutral axis, and  $\epsilon_{33}^t$  represents the elastic compliance constant.

Solving Eqs. (5) and (8) reveals that the geometric dimensions and material parameters of the piezoelectric cantilever beam have a significant impact on its electromechanical response. This observation provides a theoretical foundation for subsequent finite element modeling and simulation analysis (BAO *et al.*, 2021; CHEN *et al.*, 2020).

### 3. Structural design of PEH

#### 3.1. Dynamic test and characteristics of electric motor

The majority of PEHs are designed for general-purpose applications and are evaluated under simplified harmonic excitations. However, this approach is still far from being ready to be used in real-world applications.

It is well established that vibration-based PEHs generate maximum power when operated at their resonant frequency. A straightforward and effective solution to address this is to broaden the bandwidth of the beam's resonant frequency. The natural frequencies of the motor (shown in Fig. 2a) and the system's dynamic properties under operating conditions must be first tested and analyzed before conducting the PEH design and experiment. These parameters are critical data for conducting the structure design of the PEH (LU, 2018).

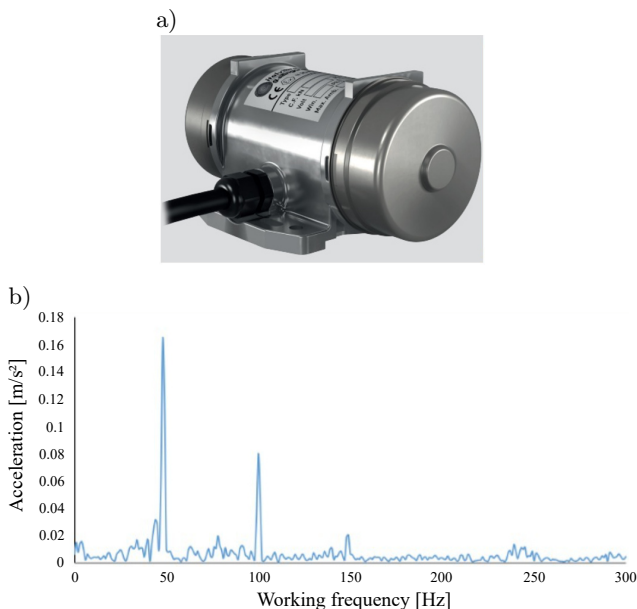


Fig. 2. a) Electric motor (Gaomeng, 2020); b) acceleration frequency spectrum under working condition.

The resonance between the PEH and the motor's natural frequency is not considered here because the

motor's modal test results, conducted earlier, indicated a very high natural frequency. The acceleration of the motor under working conditions (maximum speed) was measured, and the corresponding frequency spectrum is shown in Fig. 2b. From the figure, it can be observed that the motor exhibits several vibration peaks during operation. The peak acceleration response, which is generated by electromagnetic excitation, occurs at 50 Hz, 100 Hz, and 150 Hz – multiples of 5 Hz. These vibration frequencies generated during the operation of electrical devices, such as motors, are at the main operating frequency (50 Hz) and its harmonics. Hence, studying energy harvesting from the vibration frequencies of motors offers significant applicability.

#### 3.2. Finite element analysis

Finite element analysis (FEA) is one of the reliable methods for studying the performance of any designed system prior to its prototype development. Studies by ZHU *et al.* (2010) and AUGUSTYN *et al.* (2014) conducted parametric studies using FEA to determine the ideal system configuration. Meanwhile, studies by ABDELKEFI *et al.* (2014) and AVVARI *et al.* (2017) employed FEA to validate the experimental and analytical models of PEHs to guide further simulation. This work utilizes FEA to guide preliminary structural design and the subsequent structural parametrization, along with dynamic characteristics analysis.

##### 3.2.1. Parameter selection and analysis

Material selection and optimal structural design are crucial for energy harvesting. One important limitation of existing energy harvesting techniques is that the power output performance is subjected to the resonant frequencies of ambient vibrations, which are often random and broadband. To address this issue, researchers have focused on developing efficient PEHs using novel piezoelectric materials by adjusting the natural frequency of the harvester to match the desired vibration frequency. In terms of materials, piezoelectric materials can be categorized into natural and synthetic types. Synthetic materials are further subdivided into ceramic and polymer-based categories. The widely used piezoelectric material is PZT, known for its excellent piezoelectric properties and high dielectric constant. However, it is prone to fatigue fracture under high-frequency cyclic vibration, leading to certain limitations in its application (NIASAR *et al.*, 2020). Thus, polymer-based transducers, such as polyvinylidene difluoride (PVDF) and macro fiber composite (MFC), have gained popularity in recent years due to their flexibility, durability, and resistance to humidity (SHI *et al.*, 2017).

In this study, a laminated structure consisting of a piezoceramic plate, electrodes, and polymer materials, referred to as P-876 DuraAct patch trans-

ducer, is selected (ABDUL SATAR *et al.*, 2022). This material has the advantages of high piezoelectric coefficients and dielectric constants and can be applied onto curved surfaces or used for integration into structures. The operation mode of  $d_{31}$  is chosen, with the polarization of the electric potential perpendicular to the stress direction. In terms of the structure, a classic rectangular cantilever beam PEH is adopted, in which the piezoelectric patch is attached to the base near the fixed end, and a tip mass is attached at the free end to decrease the natural frequency.

The structural parametric study can be divided into size, shape, and topology. Size parametric study involves adjusting structural dimension parameters, such as cross-sectional area and thickness, to improve structural performance while maintaining the basic shape and topological configuration. This parametric study involves applying mathematical modeling, simulation, and specific algorithms to find the optimal combination of structural parameters that meet performance, cost, and weight constraints. Given the type and basic dimensions of the piezoelectric sensor have been determined, the research focuses on the effects of beam length and width on output voltage to achieve maximum energy production. The preliminary design of the cantilever harvester base uses an aluminum alloy with a width equal to that of the piezoelectric patch, and a thickness of 0.2 mm (ABDUL SATAR *et al.*, 2022). As discussed in Sec. 2, the experiment results indicate that the acceleration response is mainly attributed to the working frequency of the motor. Therefore, the fundamental frequency of the PEH should be tuned to match the motor's working frequency of 50 Hz. The structural design and parametric study of the PEH will be carried out using the motor's operating frequency of 50 Hz as a target operating frequency, considering both the fatigue life and energy output of the PEH beams.


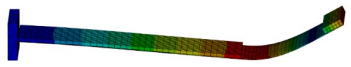

### 3.2.2. Validation of PEH

Using the piezoelectric coupling analysis module in ANSYS, the SOLID5 element, specifically designed for piezoelectric analysis, is chosen for the piezoelectric layer, while SOLID45 elements are selected for the metal layer and end mass block. Voltage degrees of freedom coupling are applied to the piezoelectric

layer as electrical constraints, and zero displacement constraints are applied to the fixed end as mechanical constraints for modal analysis. The structural natural frequencies and mode shapes can be determined using this analysis to further ascertain its size and inherent characteristics.

The FE modeling and the first three-order modes of the PEH are presented in Table 1. The first-order mode, at 50.05 Hz, aligns precisely with the frequency at which the motor operates. The second-order natural frequency is 125.90 Hz, which is much higher than the first-order mode. The red region of the vibration mode indicates the maximum deformation, while the blue region represents the minimum deformation. The first modal shape exhibits bending deformation, as shown in Table 1, where the maximum displacement occurs at the tip mass block and gradually decreases towards the fixed end. The second mode shape involves shear deformation, with the maximum deformation occurring at positions along the edge of the piezoelectric element, away from the fixed end. The third mode shape is mainly associated with twisting deformation around the horizontal axis. Unlike the bending mode, in the case of torsional vibration, the displacement at the midpoint of the cantilever beam is minimal, while the displacements on both sides in the width direction are larger.

Table 1. Modal frequency and mode shapes.

Modal order	Modal frequency [Hz]	Mode shapes
1	50.05	
2	125.90	
3	198.45	

The first-order mode of the PEH is the fundamental mode and the most appropriate for obtaining the maximum output, making it suitable for the  $d_{31}$  working mode. Hence, only the first-order mode is considered in this paper. Table 2 presents the material parameters of the PEH, along with the structural dimensions.

Table 2. Material parameters.

Parameter	Symbol	Piezoelectric patch	Substrate layer (aluminum alloy)	Mass (structure steel)
Density [kg/m <sup>3</sup> ]	$\rho$	7500	8920	7850
Young's modulus [GPa]	$E_m$	56	71.7	210
Volume [mm]	$L \times W \times t$	$60 \times 35 \times 0.8$	$90 \times 35 \times 0.2$	$35 \times 5 \times 2.5$
Poisson's ratio	$\nu$	0.36	0.33	0.31
Piezoelectric constant [C · m <sup>-2</sup> ]	$d_{31}$	$2.74 \times 10^{-10}$	—	—
Dielectric constant [nF · m <sup>-1</sup> ]	$\epsilon^t$	$3.01 \times 10^{-8}$	—	—



#### 4. Fabrication and experimental verification of PEH

The surface of the piezoelectric patch is coated with a silver electrode, and external wires are led out from here. The piezoelectric patch is bonded to an aluminum substrate using epoxy resin. Furthermore, the PEH is clamped in a rigid holder and mounted on an electromagnetic shaker to provide the base excitation, as illustrated in Fig 3.

An algorithm to generate a sinusoidal voltage signal is constructed using LabVIEW software, and this signal is supplied through an output module (NI cDAQ 9263), which is then amplified by a power amplifier to drive the shaker (Sentek BTM-100-M). The harvested voltage from the PEH and the measured acceleration are then fed back to LabVIEW software for data monitoring and analysis through the input module (NI cDAQ 9234). The control algorithm for the harvested voltage and output acceleration of the PEH, in terms of time domain and frequency response, is designed in LabVIEW software for further analysis and data validation.

The PEH experimental setup is shown in Fig. 4. The energy harvesting system operates as a coupled field of mechanical and piezoelectricity (electromechanical system). In the experiment, a signal of frequency sweep from 0 Hz to 100 Hz was supplied to

the PEH using an open-circuit sinusoidal excitation, with the input acceleration load recorded at  $3 \text{ m/s}^2$ . The resulting tip acceleration-frequency and voltage-frequency responses from this experiment are shown in Fig. 5. It can be observed that when an external excitation frequency approaches the natural frequency of the cantilever beam, the vibration acceleration and output voltage of the PEH reach their peaks. The curve of voltage peaks on both sides exhibits a symmetrical decreasing trend, which indicates that the fabricated piezoelectric oscillator has a clear natural frequency of 50 Hz.

The harmonic response analysis simulation is then carried out on the PEH model under the same excitation levels using ANSYS software. The comparison between the simulation and experimental voltages with open circuits is also illustrated in Fig. 5. This figure indicates that the peak voltage and natural frequency obtained from the simulation are nearly identical to experimental measurements with a 98.5 % correlation. The voltage drops sharply when the frequency deviates from the resonant frequency.

It should be noted that the peak voltage obtained from the FEA simulation is slightly higher than the experimental values because of the ideal boundary and loading conditions of FEA. Nevertheless, the FEA modeling results agree well with the experimental values, with the frequency differences at peak voltage values

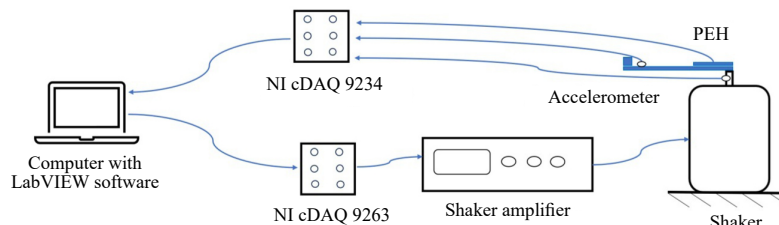


Fig. 3. Diagram of PEH experiment.

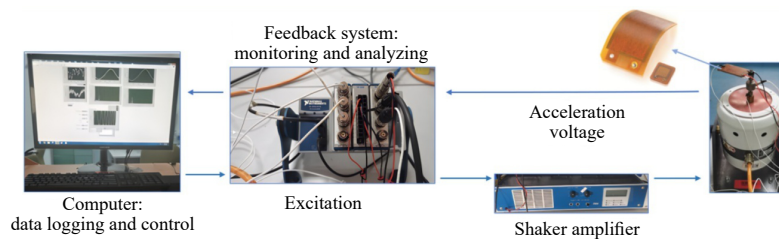


Fig. 4. Experimental setup for PEH experiment.

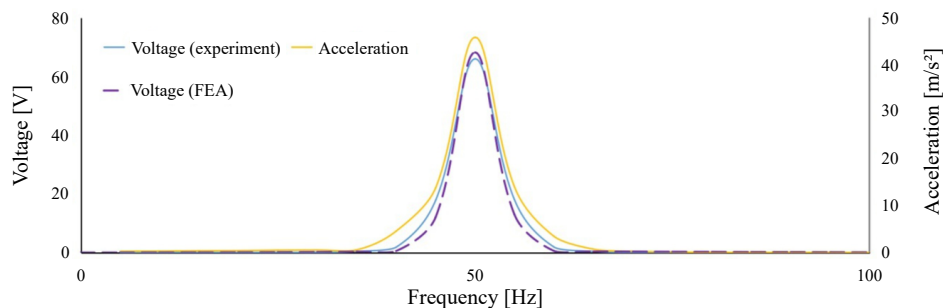


Fig. 5. Comparison of output voltage and acceleration in the frequency-domain.

falling within a range of 0.5 Hz to 1 Hz. Therefore, the FEA model is valid for the fatigue-based structural design study of the PEH.

## 5. Fatigue-based mechanism and parametric study

### 5.1. Design of structural parameters

The natural frequency and output voltage of piezoelectric cantilever beams are influenced by several factors. Therefore, it is necessary to perform a statistical analysis of various influencing factors and choose the optimal solution that achieves a natural frequency of 50 Hz, a large output voltage, and acceptable fatigue reliability. By varying the height ( $t$ ) of the tip mass, a batch of piezoelectric cantilever beams with equal areas but different aspect ratios are designed based on the results from Sec. 3, targeting a natural frequency of 50 Hz. The width and length are rounded to one decimal place to account for constraints during physical experiment.

In order to accurately ascertain the specific size and inherent characteristics, modal analysis of PEHs with the same sectional area but different shapes was conducted using ANSYS software. The voltage-frequency and stress-frequency responses of the PEHs were measured under harmonic base excitation with an acceleration of  $3 \text{ m/s}^2$ , as this work aimed to evaluate how the harvesters of different sizes performed when subjected

to identical loading conditions. The output voltage was used as the key parameter to assess the performance of the harvester, while the maximum stress in the PEH beam provided further insight into the behavior of the beam. In this study, only the stress and fatigue life of the piezoelectric patch were considered, as the fatigue strength and bending strength of the matrix material are noticeably higher than those of the piezoelectric patch.

As expected, the fundamental frequency of the designed PEHs with different aspect ratios is close to 50 Hz, as shown in the PEH voltage-frequency responses in Fig. 6a. Meanwhile, the variations in output voltage and stress versus the beam length are shown in Fig. 6b. The different sizes of PEHs combined with their natural frequency, output characteristics, and stress are summarized in Table 3. From Table 3 and Fig. 6, we can observe that both the output voltage and maximum stress exhibit an upward trend as the aspect ratio of the beams increases, with the stress increases being more noticeable. A turning point is reached at a 85 mm length and a 4.3 mm mass height, where the output voltage starts to drop, and the stress increases. The reason may be that the tip mass has an amplifying effect on the output voltage, as supported by pertinent data in (LI, LEE, 2022), and the maximum coupling effect occurring between the beam length and mass height. Subsequently, with the height of the tip mass fixed at 4.3 mm, a set of PEHs with variable lengths and widths will be constructed with a 50 Hz natural frequency as the target.

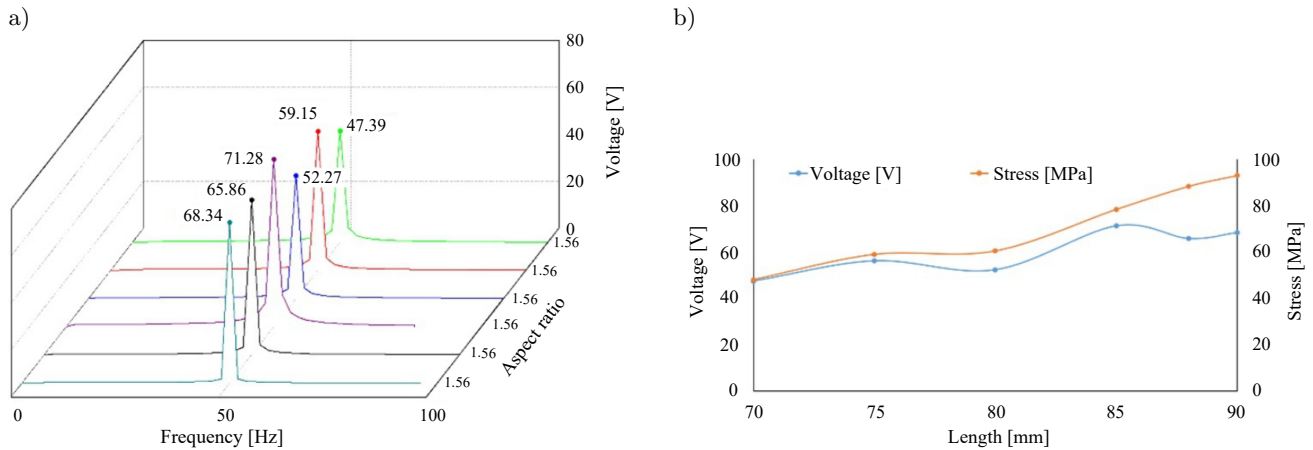


Fig. 6. a) Voltage-frequency response of different beam aspect ratios;  
b) voltage and stress induced by different beam lengths.

Table 3. Dimensions and performance parameters of Fig. 6.

Aspect ratio (L/W)	$L \times W \times t$ [mm]	Frequency [Hz]	Voltage [V]	Stress [MPa]
1.56	$70 \times 45 \times 9.2$	50.2	47.39	48.62
1.79	$75 \times 42 \times 7.2$	50.3	59.15	58.91
2.05	$80 \times 39 \times 5.6$	50.2	52.27	60.39
2.30	$85 \times 37 \times 4.3$	50.3	71.28	78.28
2.45	$88 \times 35.8 \times 3.8$ ②	50.3	65.86	88.23
2.57	$90 \times 35 \times 1.4$ ①	50.1	68.34	92.69

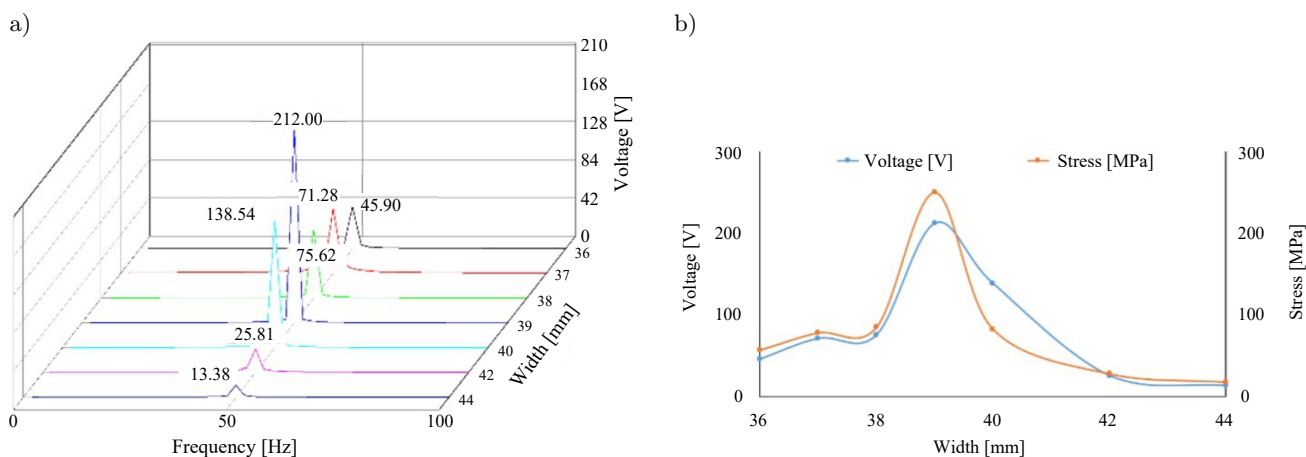


Fig. 7. a) Voltage-frequency response of different beam widths;  
b) voltage and stress induced by different beam widths.

Table 4. Dimensions and performance parameters of Fig. 7.

$L \times W \times t$ [mm]	Frequency [Hz]	Voltage [V]	Stress [MPa]
$84.6 \times 36 \times 4.3$	50.2	45.90	57.17
$85 \times 37 \times 4.3$ ④	50.3	71.28	78.28
$85.2 \times 38 \times 4.3$	50.3	75.62	85.43
$85.5 \times 39 \times 4.3$	50.1	212.00	249.71
$86.2 \times 40 \times 4.3$ ③	50.1	138.54	82.66
$86.6 \times 42 \times 4.3$	49.9	25.81	28.14
$89.8 \times 44 \times 4.3$	49.8	13.38	17.92

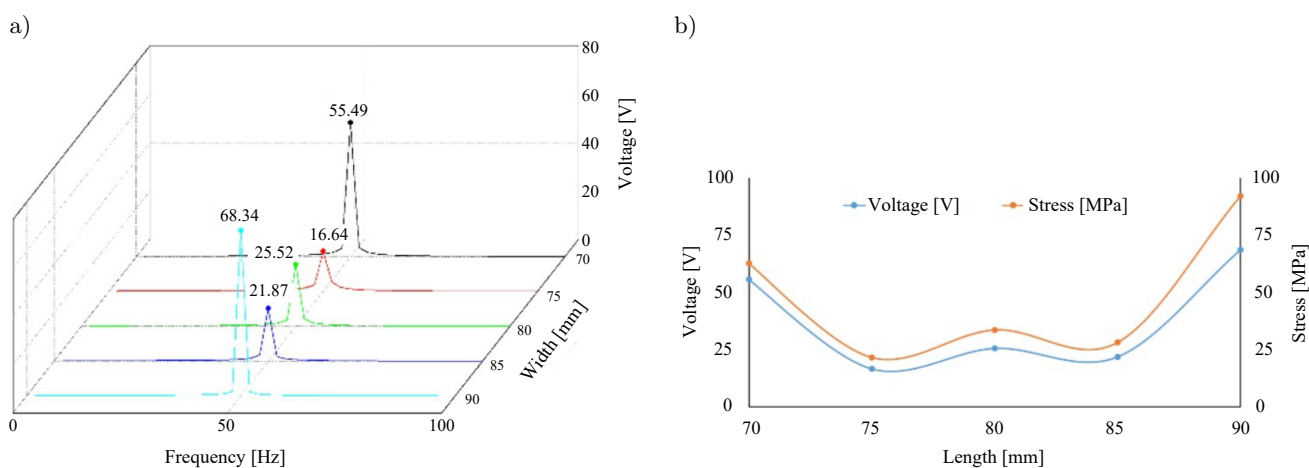


Fig. 8. a) Voltage-frequency response of different beam lengths;  
b) voltage and stress induced by different beam lengths.

Table 5. Dimensions and performance parameters of Fig. 8.

$L \times W \times t$ [mm]	Frequency [Hz]	Voltage [V]	Stress [MPa]
$90 \times 35 \times 1.4$	50.1	68.34	92.69
$85 \times 35 \times 1.9$	49.8	21.87	28.34
$80 \times 35 \times 3.2$	50.2	25.52	33.52
$75 \times 35 \times 4.8$	50.4	16.64	21.56
$70 \times 35 \times 5.9$ ⑤	50.1	55.49	62.51



The voltage-frequency responses of the designed PEHs with different beam widths are shown in Fig. 7a, and the variations in output voltage and stress versus beam width, using the same tip mass, are shown in Fig. 7b. The specific dimensions and related characteristics of the beam are shown in Table 4. From Table 4 and Fig. 7, we can conclude that as the length and width increase, both the voltage and stress initially grow and subsequently drop. The voltage is at its maximum when the width is 39 mm, while the stress is also relatively significant, even exceeding the material's yield limit of 108 MPa (WU, 2013). The output voltage is relatively high when the width is 40 mm, but the absolute value of the stress is lower than the voltage, which meets the PEH selection criteria. Finally, by using a fixed width of 35 mm (the minimum width, equal to the width of the PEH), with the beam length and mass height as variables, a set of PEHs has been investigated, as shown in the voltage-frequency responses in Fig. 8a, and the variations in voltage and stress versus beam length are shown in Fig. 8b. Specific dimensions and related characteristics are listed in Table 5. From these figures and table, the results indicate that with the increase of the beam length and the decrease in the mass height, both output voltage and stress initially decrease and then increase. When the beam is at its minimum length of 70 mm, the output characteristics are significantly influenced by the mass block; on the other hand, when the mass height is at its minimum of 1.4 mm, the output characteristics are primarily influenced by the beam length.

Based on the foregoing analysis, five beams, labeled ① to ⑤, are chosen for further fatigue life analysis. These beams are chosen based on the criteria of having a higher output voltage and a maximum stress smaller than the material's yield strength limit.

### 5.2. Prediction of fatigue life

The main methods for fatigue life analysis include the nominal stress method and local stress-strain methods (ZHANG *et al.*, 2014). The former involves estimating life based on the  $S-N$  curve using fatigue cu-

mulative damage theory, which is appropriate for high-cycle fatigue failures with cycles greater than  $10^4$ . The latter calculates the crack initiation life using the local stress-strain approach and predicts crack propagation life using fracture mechanics, making it suitable for low-cycle fatigue failures with cycles less than  $10^4$  (SALAZAR *et al.*, 2021). Both methods are based on the fatigue characteristics of materials and fatigue cumulative damage theory. Since piezoelectric transducers are subject to high-cycle fatigue, the nominal stress method approach is used in this study.

The fundamental principle of performing fatigue analysis using ANSYS software is to use FEA to obtain the stress and strain distribution of a structure under external periodic loads. These results are then combined with the material fatigue performance curve, and fatigue theory is applied to calculate the fatigue life distribution of the components. This process aids in predicting potential failures of structural components due to fatigue over long durations of operation. Stress-life curves for piezoelectric patch materials are not available in the ANSYS material library. Therefore, it is necessary to set up the fatigue properties of piezoelectric patch materials by generating stress-life curves using parameters provided by the manufacturer, such as elastic modulus and fatigue limit, which allows for the simulation and analysis of the fatigue behavior of piezoelectric patch transducer.

The analysis is conducted by applying the identical constant excitation equal to the initial resonant frequency to five PEHs. After obtaining the required parameters and calculating the stress distribution and fatigue life, the simulation results indicate that the maximum stress occurs at the root of the cantilever beam. Stress concentration and early fatigue failure occur at both ends of the cantilever beam, as illustrated in the fatigue life contour map for the piezoelectric patch layer in Fig. 9a and 9b. The blue areas represent the maximum fatigue life, while the red areas indicate the minimum fatigue life that the PEH can withstand. The yellow circles in Fig. 9c illustrate the specific locations on the PEH that are prone to fatigue damage, based on the simulation. This conclusion can

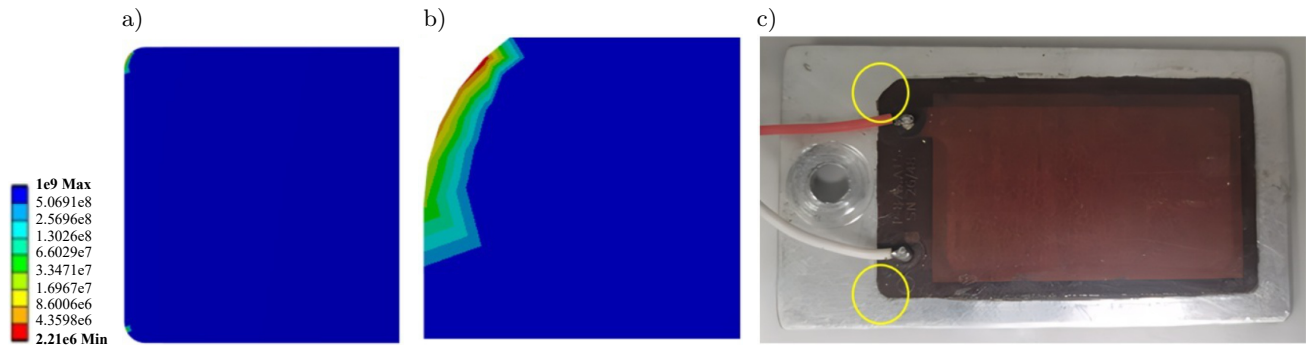


Fig. 9. a)–b) FE simulation results; c) actual PEH beam under study.

Table 6. Fatigue life of beams.

Serial number	Beam	Output voltage	Fatigue life
①	$90 \times 35 \times 1.4$	68.34	$1.76 \times 10^7$
②	$88 \times 35.8 \times 3.8$	65.86	$1 \times 10^9$
③	$86.2 \times 40 \times 4.3$	138.54	$2.21 \times 10^6$
④	$85 \times 37 \times 4.3$	71.28	$1.03 \times 10^7$
⑤	$70 \times 35 \times 5.9$	55.49	$1 \times 10^9$

serve as a reference for future structural parameters and optimization studies.

For typical fatigue analysis, if a specimen does not fail after  $10^7$  stress cycles, it is assumed that the specimen will not fail even after an infinite number of stress cycles (WANG *et al.*, 2021). As shown in Table 6, it can be observed that under the same external loads, beams ①, ②, ④, and ⑤ have the fatigue life exceeding  $10^7$  cycles, indicating that fatigue failure is unlikely to occur. For a certain natural frequency of the beams, both output voltage and fatigue life are influenced by the combined effects of the mass block and the structural length-to-width ratio, and this influence is non-linear. In general, the larger the output voltage, the shorter the lifespan. Therefore, when designing a PEH for a specific frequency, it is critical to consider the coupling effects of the mass block and aspect ratio, while balancing the trade-off between output voltage and fatigue life to select the best solution that fits the actual vibration environment. In terms of the motor usage environment, that is for indoor electrical devices (such as machine tools), design schemes ① and ④ are recommended. They maximize output voltage while meeting the fatigue life requirements. For outdoor application, with an uncertain vibration environment (such as automotive), design scheme ② is recommended to ensure the cantilever beam has a sufficient safety margin to withstand extreme external loads. If space is limited, design scheme ⑤ can be considered. If the output power of the chosen beam is insufficient to meet certain requirements, increasing the surface area of the piezoelectric layer can be an alternative solution. Option ③ is suitable for situations with high output power demands and a low requirement for safety margin.

## 6. Conclusion

Long-term vibration loading at a constant amplitude of excitation in a PEH can induce fatigue damage at the root of the cantilever beam in the long run. In this study, three sets of PEHs with distinct fixed and variable values were designed for an electric motor with a 50 Hz vibration frequency. After comprehensively considering the output voltage and fatigue life of the piezoelectric cantilever beam, suitable design solutions for various environments and operational conditions were investigated. The conclusions are summarized as follows:

- The dimensions of the beam and the weight of mass will result in the optimal solution for output voltage and fatigue life at the maximum coupling effect position for a PEH with specific natural frequency of 50 Hz. When designing the structure of the PEH beam, output voltage should not be the sole design objective; instead, comprehensive consideration of both the output voltage and the fatigue life of the piezoelectric layer is necessary.
- Five optimized design schemes with a frequency of 50 Hz were selected in this study, and these are recommended for application in different operational environments and for varying design purposes.
- The structural parametric study of the PEH with a specific natural frequency of 50 Hz, along with the determination and analysis of the optimal scheme, provides a simple and effective method for the structural optimization design of PEH beams.

Based on these conclusions, it is necessary to conduct further research to determine the optimal parameters for the elastic beam in PEH. The fundamental correlations between the parameters and structural properties, as obtained in this study, are shown in Table 7, which will be useful as a reference for future PEH design research.

Table 7. Parameters correlation analysis in designing PEH.

Parameters	Length	Width	Mass
Relationship with structural frequency	Negative correlation	Positive correlation	Negative correlation
Relationship with output voltage	Positive correlation	Negative correlation	Positive correlation

## FUNDING

The authors would like to thank the Ministry of Higher Education in Malaysia for the Fundamental Research Grant Scheme (FRGS) under project code FRGS/1/2021/TK0/USM/03/6, and the Science and Technology Research Program of Chongqing Municipal Education Commission (grant no. KJQN 202404004).

## References

1. ABDELKEFI A., BARSALLO N., TANG L., YANG Y., HAJJ M.R. (2014), Modeling, validation, and performance of low-frequency piezoelectric energy harvesters,

- Journal of Intelligent Material Systems and Structures*, **25**(12): 1429–1444, <https://doi.org/10.1177/1045389X13507638>.
2. ABDUL SATAR M.H., MURAD A.F., AHMAD MAZLAN A.Z. (2022), Characterization of piezoelectric patch material with hysteresis, saturation, creep, and vibration nonlinearity effects and its application to the active vibration suppression for cantilever beam, *Journal of Vibration and Control*, **28**(3–4): 476–489, <https://doi.org/10.1177/1077546320980571>.
  3. AUGUSTYN E., KOZIEŃ M.S., PRĄCIK M. (2014), FEM analysis of active reduction of torsional vibrations of clamped-free beam by piezoelectric elements for separated modes, *Archives of Acoustics*, **39**(4): 639–644, <https://doi.org/10.2478/aoa-2014-0069>.
  4. AVVARI P.V., YANG Y., SOH C.K. (2017), Long-term fatigue behavior of a cantilever piezoelectric energy harvester, *Journal of Intelligent Material Systems and Structures*, **28**(9): 1188–1210, <https://doi.org/10.1177/1045389X16667552>.
  5. BAO B., WANG Q., WU N., ZHOU S. (2021), Hand-held piezoelectric energy harvesting structure: Design, dynamic analysis, and experimental validation, *Measurement*, **174**: 109011, <https://doi.org/10.1016/j.measurement.2021.109011>.
  6. CHEN C., SHARAFI A., SUN J.Q. (2020), A high density piezoelectric energy harvesting device from highway traffic – Design analysis and laboratory validation, *Applied Energy*, **269**: 115073, <https://doi.org/10.1016/j.apenergy.2020.115073>.
  7. FENG Y., LIU W., GAO M., CHEN H., LU Q. (2023), Analysis of electromechanical response and fatigue life of piezoelectric cantilever beam [in Chinese], *Failure Analysis and Prevention*, **18**(3): 184–190, <http://doi.org/10.3969/j.issn.1673-6214.2023.03.007>.
  8. Gaomeng (n.d.), Shanghai GOM Testing & Technical Co., Ltd., <https://www.gaomengce.com> (access: 1.05.2024).
  9. LI T., LEE P.S. (2022), Piezoelectric energy harvesting technology: From materials, structures, to applications, *Small Structures*, **3**(3): 2100128, <https://doi.org/10.1002/ssstr.202100128>.
  10. LU Q. (2018), *Structure design and electro-mechanical performance analysis of vibration piezoelectric composite energy harvester*, Ph.D. Thesis, Harbin Institute of Technology.
  11. NIASAR E.H.A., DAHMARDEH M., GOOGARCHIN H.S. (2020), Optimization of a piezoelectric energy harvester considering electrical fatigue, *Journal of Intelligent Material Systems and Structures*, **31**(12): 1443–1454, <https://doi.org/10.1177/1045389X20923086>.
  12. PANDA S. *et al.* (2022), Piezoelectric energy harvesting systems for biomedical applications, *Nano Energy*, **100**: 107514, <https://doi.org/10.1016/j.nanoen.2022.107514>.
  13. RAFIQUE S., BONELLO P. (2010), Experimental validation of a distributed parameter piezoelectric bimorph cantilever energy harvester, *Smart Materials and Structures*, **19**(9): 094008, <https://doi.org/10.1088/0964-1726/19/9/094008>.
  14. ROUNDY S. *et al.* (2005), Improving power output for vibration-based energy scavengers, *IEEE Pervasive Computing*, **4**(1): 28–36, <https://doi.org/10.1109/MPRV.2005.14>.
  15. SALAZAR R., LARKIN K., ABDELKEFI A. (2021), Piezoelectric property degradation and cracking impacts on the lifetime performance of energy harvesters, *Mechanical Systems and Signal Processing*, **156**: 107697, <https://doi.org/10.1016/j.ymssp.2021.107697>.
  16. SEZER N., KOÇ M. (2021), A comprehensive review on the state-of-the-art of piezoelectric energy harvesting, *Nano Energy*, **80**: 105567, <https://doi.org/10.1016/j.nanoen.2020.105567>.
  17. SHI Y., HALLETT S.R., ZHU M. (2017), Energy harvesting behaviour for aircraft composites structures using macro-fibre composite: Part I – Integration and experiment, *Composite Structures*, **160**: 1279–1286, <https://doi.org/10.1016/j.compstruct.2016.11.037>.
  18. WANG J., QIN X., LIU Z., DING G., CAI G. (2021), Experimental study on fatigue degradation of piezoelectric energy harvesters under equivalent traffic load conditions, *International Journal of Fatigue*, **150**: 106320, <https://doi.org/10.1016/j.ijfatigue.2021.106320>.
  19. WANG S.L., SONG J., ZHAO X.Y. (2019), Research on energy recovery device of electric vehicle seat based on piezoelectric effect, [in:] *2019 13th Symposium on Piezoelectricity, Acoustic Waves and Device Applications (SPAWDA)*, <https://doi.org/10.1109/SPAWDA.2019.8681810>.
  20. WU X. (2013), *The fatigue analysis and experimental research of piezoelectric pump with single chip vibrator*, Master Thesis, University of Jilin.
  21. ZHANG M., MENG Q., WANG H. (2014), Fatigue analysis for cantilever piezoelectric vibration energy harvester.
  22. ZHANG Q., LIU Z., JIANG X., PENG Y., ZHU C., LI Z. (2022), Experimental investigation on performance improvement of cantilever piezoelectric energy harvesters via escapement mechanism from extremely low-frequency excitations, *Sustainable Energy Technologies and Assessments*, **53**(Part B): 102591, <https://doi.org/10.1016/j.seta.2022.102591>.
  23. ZHU M., WORTHINGTON E., TIWARI A. (2010), Design study of piezoelectric energy-harvesting devices for generation of higher electrical power using a coupled piezoelectric-circuit finite element method, *IEEE Transactions on Ultrasonics, Ferroelectrics, and Frequency Control*, **57**(2): 427–437, <https://doi.org/10.1109/TUFFC.2010.1423>.